



Open Archive Toulouse Archive Ouverte (OATAO)

OATAO is an open access repository that collects the work of Toulouse researchers and makes it freely available over the web where possible.

This is an author-deposited version published in: <http://oatao.univ-toulouse.fr/>
Eprints ID : 2443

To link to this article :

URL : <http://dx.doi.org/10.1016/j.surfcoat.2007.04.073>

To cite this version : Sarantopoulos, Christos and Gleizes, Alain and Maury, Francis (2007) *[Chemical vapor infiltration of photocatalytically active TiO₂ thin films on glass microfibers.](#)* Surface and Coatings Technology, vol. 201 (n° 22 - 23). pp. 9354-9358. ISSN 0257-8972

Any correspondence concerning this service should be sent to the repository administrator: staff-oatao@inp-toulouse.fr

Chemical vapor infiltration of photocatalytically active TiO₂ thin films on glass microfibers

Christos Sarantopoulos*, Alain N. Gleizes, Francis Maury

CIRIMAT, CNRS/INPT/UPS, ENSIACET, 118 Route de Narbonne, 31077 Toulouse cedex 4, France

Abstract

Due to the high diffusivity of the chemical species, chemical vapor infiltration (CVI) is a suitable process for the conformal coverage of objects with large dimensions and complex shape geometry. Its large scale capacity and high reproducibility have made the technique favorable for the deposition of non-oxide ceramics. There are few works on other materials and metal-organic compounds are rarely used as molecular precursors. In this study we focus on the deposition of anatase thin films on substrates with large surface area (microfibers) for photocatalytic air treatment systems. Titanium tetra-isopropoxide (TTIP) was used as precursor without additional oxygen source. Using low mole fractions ($26\text{--}124 \times 10^{-5}$) and low deposition temperatures (300–400 °C), a relatively good thickness uniformity was obtained along the reactor axis. Infiltration experiments were achieved in this temperature range and under 1 Torr for high TTIP diffusivity ($110\text{--}146 \text{ cm}^2 \text{ s}^{-1}$) and low initial Thiele modulus (0.11–0.13) values. Photocatalytic activity of TiO₂ coated glass microfiber samples depends on the film morphology, average thickness and infiltration efficiency. It is shown that this latter parameter plays a major role due to the increase of active surface area.

Keywords: CVI; Infiltration; Microfibers; Titanium dioxide; Anatase; Photocatalysis

1. Introduction

Chemical vapor infiltration (CVI) is an efficient process for producing ceramic-matrix composites materials such as SiC [1] and TiC [2], pyro-C [3] or refractory metal-matrix such as Re [4]. In particular, isothermal isobaric CVI is a well studied process applied in industrial scale but it is characterized by low deposition rates and long infiltration times. For these reasons many studies were focused on theoretical and numerical modeling to optimize the densification rates [5]. To our knowledge, CVI has not been used for the growth of oxide ceramics on glass fibers. Furthermore, the use of metal-organic precursors in CVI is rare. This is generally considered challenging because of their high reactivity at rather low temperatures which complicates the control of the deposition rate. Another reason is the low diffusivity of large metal-organic molecules as titanium tetra-isopropoxide (TTIP) through porous structures. Smaller and more stable precursors as halides TiCl₄ [2] or ReCl₅ [4]

are preferred to infiltrate substrates with large dimensions. However metal-organic precursors, such as Si(C₂H₅)₄ for instance, were successfully used [6]. Until now almost all works for immobilizing TiO₂ thin films on inorganic (glass) microfibers are using the dip coating method in a solution containing titania sol and then annealing for many hours at relatively high temperatures (500 °C) to obtain crystallization of nanoparticles [7]. Despite important advantages (simplicity, cheap process), TiO₂ films obtained by this technique can exhibit poor adhesion [8], low conformal coverage of the fibers, and their microstructure cannot be changed as conveniently as in CVD. This can be a major drawback to produce advanced supported photocatalysts.

Carrying on a research program on CVD TiO₂ for various applications [9–11], we were interested in studying the use of metal-organic source like TTIP in an isothermal, isobaric CVI process in order to functionalize (not to densify) with a TiO₂ thin film porous substrates of complex geometry, like glass microfiber tissues. Our goal is to produce uniform TiO₂ thin films featuring high specific surface area, suitable for photocatalytic air treatment systems. Glass microfiber tissue is a

* Corresponding author. Tel.: +33 5 62 88 56 66; fax: +33 5 62 88 56 00.
E-mail address: christos.sarantopoulos@gmail.com (C. Sarantopoulos).

convenient support for applications in gas treatment. It offers flexibility, large surface area compared to flat substrates, glass beads or honeycomb type supports used until now for photocatalytic applications. Furthermore, it is transparent in a large domain of light spectrum including UV-A.

In the present work, we study the influence of the growth process parameters to improve the deposition uniformity, infiltration efficiency and conformal coverage through porous substrates of relatively large dimensions at the laboratory scale. Comparisons between the CVI conditions leading to the most promising microstructure and those giving the best infiltration efficiency lead us to a compromise for the preparation conditions of supported photocatalysts.

2. Experimental

2.1. Films preparation

TiO₂ films were grown in an isothermal, isobaric, horizontal low pressure-CVD reactor (45 mm in diameter). Two types of substrates were used. For preliminary experiments, flat borosilicate glass and Si(100) wafers were used as previously reported [12]. For the infiltration runs, “E-glass” type tissue (30 g m⁻²), obtained from C.Y.S. Grp. Composites, was used as support. It is a high void medium (~90% porosity) with pore diameter of 30–100 μm generated by randomly weaved fibers (12 μm average diameter). This tissue exhibits relatively large surface area (0.13 m² g⁻¹). It is stable up to 800 °C and the chemical composition is: SiO₂ 54%, Al₂O₃ 15%, CaO 17%, MgO 5%, R₂O <0.8%, B₂O₃ 8%. Prior to CVI runs, it was thermally treated at 500 °C under air stream in order to remove the dressing thin organic film. Three to eleven tissue pieces (20 × 100 mm²) were stacked for infiltration experiments. They were maintained between two aluminum frames. This assembly was placed along the reactor axis (*z*) in the isothermal zone at 16 cm from the entrance. Pure nitrogen (99.9992%) was used both as a carrier gas through the TTIP bubbler and as a dilution gas (580 sccm). The flow rates were monitored by mass flow controllers. The TTIP mole fraction (χ_{TTIP}) was controlled by the temperature of the TTIP bubbler (21–60 °C) and determined by the TTIP weight loss after the CVI experiment. The total pressure was maintained constant using a vacuum pump equipped with an automatic control system. The growth temperature (300–600 °C) was measured with a thermocouple K plugged into the sample holder. Film thickness (or TiO₂ mass) was controlled by varying the deposition time (180–300 min).

2.2. Films characterization

Film crystallinity was determined by X-ray diffraction (XRD; θ – θ geometry). Microstructure, grain size and film thickness were analyzed by scanning electron microscopy (SEM) equipped with an X-ray energy dispersive spectroscopy analyzer (EDS). The thickness uniformity along the *z* axis and the infiltration depth through stacked glass fiber tissues were studied by measuring the Ti/Si EDS intensity ratios. TiO₂ film specific surface area was measured by B.E.T analysis.

2.3. Photocatalytic test

The photocatalytic activity of TiO₂ films was evaluated from the initial decomposition rate of a dye compound in a batch reactor. Glass tissue samples (20 × 30 × 1 mm³ and 20 × 100 × 1 mm³) coated with TiO₂ were immersed into an Orange G aqueous solution (10⁻⁵ mol l⁻¹). The supported photocatalyst and 25 cm³ of the dye solution were placed into a quartz vessel (28.8 cm³) transparent to wavelengths >290 nm, and irradiated at 365 nm with a UV-A lamp (HPLN Philips 125 W) under irradiance of 1.05 mW cm⁻². All solutions were first agitated for 1 h in the dark to assure equilibrium of adsorption with the photocatalyst. The concentration was determined by measuring the absorbance of Orange G at 480 nm, using a UV/Vis spectrophotometer and applying the Beer–Lambert law. Photocatalytic degradation generally follows a Langmuir–Hinshelwood mechanism with the rate *r* being proportional to the relative coverage θ . In case of low initial concentrations of the dye (<10⁻³ mol l⁻¹), the term *K*·*C* can be neglected with respect to 1 and the rate becomes first order,

$$r = k \cdot \theta = k \cdot K \cdot C = k_a \cdot C \quad (1)$$

where *k* is the true rate constant, *K* is the adsorption constant and *k_a* is the apparent rate constant. The initial decomposition rate *r*₀ was determined for the first 30 min of the reaction from the slope of the gradient of the concentration *C* of Orange G as a function of time.

3. Results and discussion

3.1. Growth kinetics

Homogeneous infiltration into the pores of a preform can only be achieved if the values of the initial Thiele modulus are low [5]. This means that low growth rates, high diffusivity and high precursor concentrations are required to avoid a starving reactor mode. To achieve infiltration in an isothermal, isobaric reactor configuration, very low precursor conversion rates and long deposition times have to be achieved. In general, the overall process must be controlled by surface chemical reactions involving the precursor and not by mass transport limitation of the reactive species through the pores of the preform. For evaluating the infiltration efficiency, (i) the kinetic regime, (ii) the rate constant of the overall chemical reaction, (iii) the diffusion coefficient of the reactive species and (iv) the pore geometry must be known.

In these objectives, preliminary LPCVD runs were performed to optimize the growth rate uniformity along the reactor *z* axis on flat substrates. A relatively good uniformity was obtained at low temperatures (300–400 °C), low TTIP mole fractions (26–124 × 10⁻⁵) and high gas flow rates. For deposition on glass fiber tissues, the thickness gradient along the reactor was estimated on the external tissue (top) of the assembly. With moderate TTIP mole fractions in the range 124–500 × 10⁻⁵, the thickness gradient is quite smooth at 300 °C and more pronounced at 400 °C (Fig. 1).

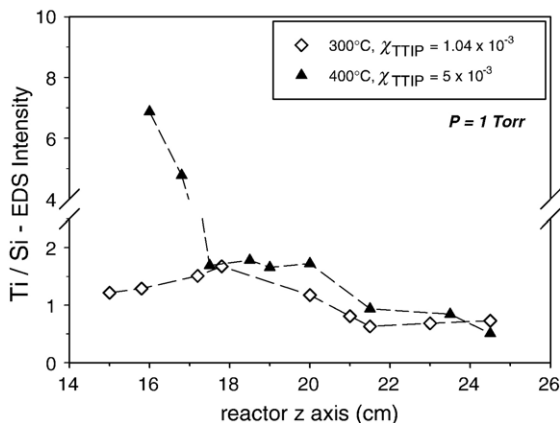


Fig. 1. Influence of the growth temperature on the axial thickness uniformity of TiO_2 films deposited on the external tissue (top) of a 3-stacked tissue assembly. The relative thickness is estimated from the Ti/Si intensity ratio of EDS signals.

Feed rate-limited deposition usually provides a rate with weak temperature dependence as observed for low TTIP mole fractions (7.6×10^{-5}). For higher TTIP mole fractions (26 and 103.5×10^{-5}), two regimes show up (Fig. 2): between 300 and 400 °C the deposition rate increases with the temperature suggesting a surface reaction-limited deposition; above 400 °C the rate depends weakly on the temperature, giving evidence for a diffusion controlled regime. Similar variations were previously reported [13].

In the kinetically controlled temperature range (300–400 °C), the deposition rate increases linearly with the TTIP mole fraction suggesting a first order reaction. This is in good agreement with literature works [13], even if a second order reaction was reported for deposition experiments under high vacuum (no carrier gas) [14]. Because of different local growth conditions resulting from various reactor designs, discrepancies are observed for the apparent activation energy values. The value found here (93 kJ mol^{-1}) is in the literature range [9,10,15]. The infiltration experiments were performed at

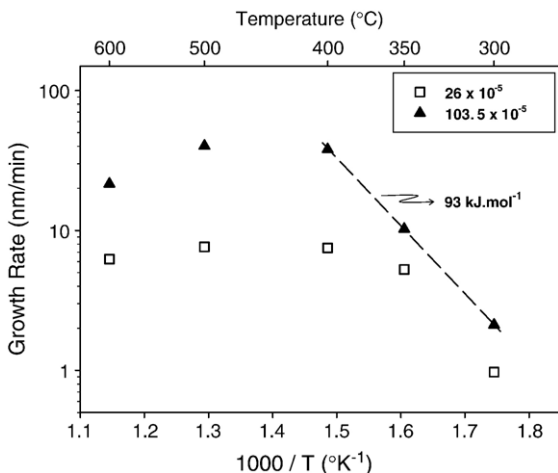


Fig. 2. Arrhenius plot for the growth rate of TiO_2 on Si(100) substrates from TTIP ($P=20 \text{ Torr}$, $\chi_{\text{TTIP}}=26 \times 10^{-5}$ and 103.5×10^{-5}).

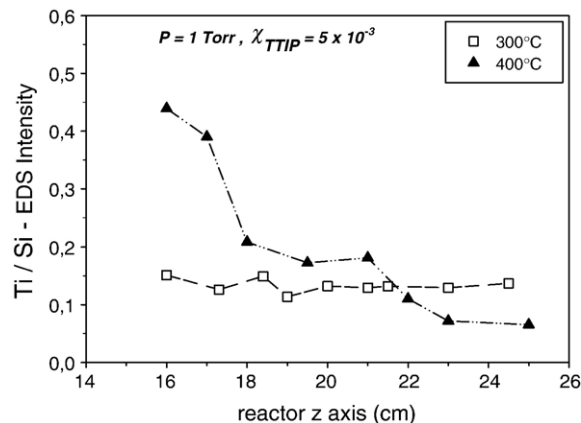


Fig. 3. Influence of the deposition temperature on the infiltration efficiency analyzed by film thickness uniformity on the middle tissue of a 3-stacked tissue assembly. The relative thickness is estimated from the Ti/Si intensity ratio of EDS signals.

low temperatures (300–400 °C) with a total pressure in the range 1–20 Torr.

3.2. Infiltration efficiency

Infiltration efficiency was first studied on an assembly (1 cm thick) constituted of 11 stacked tissues. Initial Thiele modulus was calculated for a first order reaction according to the formula proposed by Chang et al. [5]. When operating at 20 Torr and

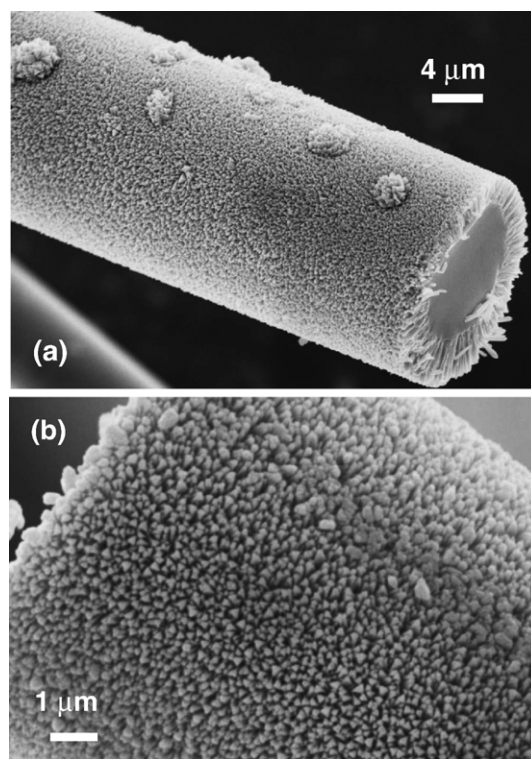


Fig. 4. Morphology of infiltrated TiO_2 films on glass fibers. This columnar and porous morphology provides a relatively high specific surface area ($17 \text{ m}^2 \text{ g}^{-1}$) and is suitable for photocatalysis ($P=20 \text{ Torr}$, $T=400 \text{ °C}$, $\chi_{\text{TTIP}}=7.6 \times 10^{-5}$ or 26×10^{-5}).

400 °C ($\chi_{\text{TTIP}}=26\text{--}124\times 10^{-5}$), infiltration was poor for the tissues in the middle of the stack. Decreasing the number of stacked tissues while keeping constant the pressure, did not improve the infiltration. By decreasing the pressure from 20 to 1 Torr, TTIP diffusion coefficient in N_2 increased from 7.3 to $146\text{ cm}^2\text{ s}^{-1}$ and as a result, TiO_2 grew on the middle tissue too. At 400 °C ($\chi_{\text{TTIP}}=5\times 10^{-3}$), infiltration is satisfactory but a thickness gradient along the z axis is observed due to precursor depletion. The infiltration is more effective at 300 °C (Fig. 3). TTIP mole fraction plays an important role on infiltration efficiency. Indeed, at 300 °C and 1 Torr, infiltration is improved by increasing TTIP mole fraction. Infiltration efficiency is defined by the ratio between the Ti/Si EDS intensity ratio on the middle tissue and that on the external tissue for a given position along the z axis (16 cm from reactor entrance). For $\chi_{\text{TTIP}}=26$, 124 and 500×10^{-5} , the infiltration efficiency raises from 0.05 to 0.25 and to 1 (± 0.1), respectively. Tissue mass gain measurements of TiO_2 are in agreement with these observations.

3.3. Morphology and film microstructure

Films obtained at 400 °C, 20 Torr exhibit a columnar morphology (Fig. 4). A similar growth mode was previously observed on flat substrates [9,12]. Due to the surface curvature,

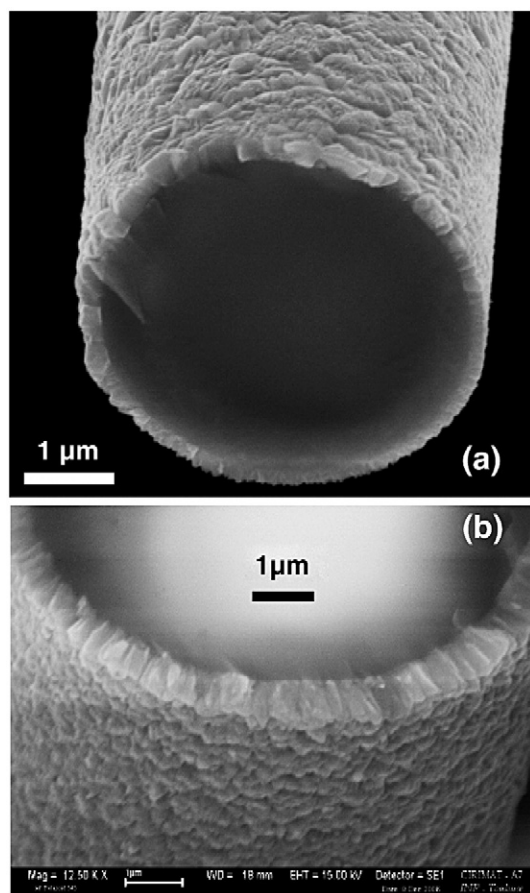


Fig. 5. Influence of the deposition temperature on the morphology of infiltrated TiO_2 films on glass fibers using: (a) $P=1$ Torr, $T=300$ °C, $\chi_{\text{TTIP}}=10^{-3}$ or 5×10^{-3} ; (b) $P=1$ Torr, $T=400$ °C, $\chi_{\text{TTIP}}=5\times 10^{-3}$.

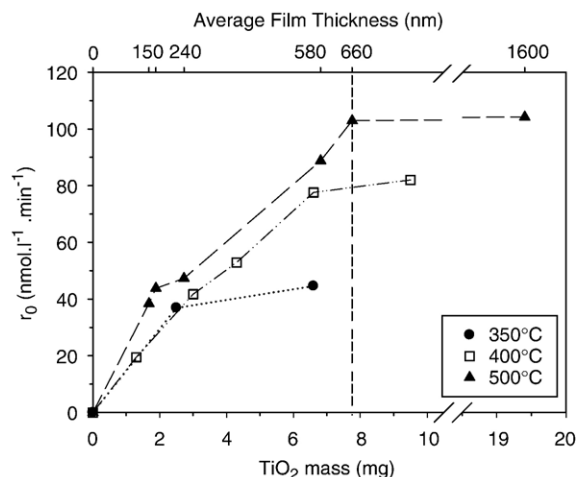


Fig. 6. Photocatalytic initial decomposition rate r_0 of Orange G aqueous solutions using single glass tissue uniformly coated with TiO_2 thin films of various average thicknesses (mass of photocatalyst) and grown at different temperatures ($\chi_{\text{TTIP}}=7.6\times 10^{-5}$ and 26×10^{-5} ; $P=20$ Torr; sample size $20\times 32\times 1\text{ mm}^3$).

the spacing between the columns is larger on microfibers than on flat glass surfaces. Porosity was 40% for a $1.5\text{ }\mu\text{m}$ thick film on flat glass [16]. The porosity of deposits on microfibers could not be measured at this stage but we may assume that it is higher than 40%. The specific surface area of $1\text{--}3\text{ }\mu\text{m}$ thick films on glass fibers was found equal to $17\pm 0.1\text{ m}^2\text{ g}^{-1}$. This particular morphology is beneficial for photocatalytic applications. However under these growth conditions the infiltration efficiency is low. For the best CVD parameters (300 °C, 1 Torr), a good TiO_2 coverage of the glass fibers was observed but the films exhibit a compact granular morphology constituted of grains with an average size of 250 nm (Fig. 5a). The corresponding surface area drops down to $1.0\pm 0.1\text{ m}^2\text{ g}^{-1}$. At the same pressure, the growth turns more columnar at 400 °C resulting in a higher porosity (Fig. 5b). These conditions could be a good compromise.

3.4. Photocatalytic activity

Fig. 6 shows the variation of the initial decomposition rate r_0 as a function of TiO_2 deposited mass for different growth temperatures. The samples were prepared under 20 Torr using a low TTIP mole fraction (7.6×10^{-5}), except for the $1.6\text{ }\mu\text{m}$ thick one that was grown with $\chi_{\text{TTIP}}=26\times 10^{-5}$ (poorer infiltration conditions). The average film thickness was calculated assuming a total and uniform coverage of the microfibers by the TiO_2 film. All films exhibit the anatase structure except those grown at 500 °C which contains traces of rutile. The initial decomposition rate r_0 increases almost linearly with film thickness up to a critical thickness of ca. 600 nm and then tends to a plateau. Previous work on flat glass substrates has shown that UV-A light absorption was saturated for film thickness of $1\text{--}1.5\text{ }\mu\text{m}$ [16]. This critical thickness is significantly higher than the threshold at 600 nm observed for the photocatalytic activity of deposits on microfibers. Therefore, the photocatalytic reaction rate for the films on microfibers is not limited by

Table 1

Comparison between CVI growth conditions and the main features of the samples consisting of a 3-stacked glass tissue assembly ($20 \times 100 \times 3 \text{ mm}^3$)

Sample series	# 1	# 2	# 3
Pressure (Torr)	20	1	1
Temperature ($^{\circ}\text{C}$)	400	300	400
TTIP mole fraction (10^{-5})	7.6–26	124–500	500
Morphology ^a (columnar, porosity)	+++	+	++
Axial thickness uniformity ^a	+++	+++	++
Infiltration ^a	+	+++	++
Thiele modulus	1.5	0.11	0.13
Normalized photocatalytic activity ($\text{nmol l}^{-1} \text{ min}^{-1} \text{ mg}^{-1}$)	5.2 ^b	56 ^c	9.8 ^c

^a+++ excellent; ++ good; + poor.

^bExternal (top) tissue.

^cMiddle tissue.

light absorption. It is more dependent on the microstructural features (porosity) for comparable amounts of deposited photocatalyst.

Grown at 350°C , TiO_2 films show a higher compactness resulting in lower photocatalytic efficiency. Films grown in the temperature range $400\text{--}500^{\circ}\text{C}$, consist of well formed, regular and sharp columns. Therefore, their porosity is very likely higher than that of 40% found on flat substrates [16]. They exhibit an enhanced photocatalytic activity compared to films grown at 350°C (Fig. 6). The best behavior, observed at 500°C , is in good agreement with a previous work [17] and can be explained by better crystallization and lower carbon contamination. Preliminary photocatalytic tests have also been carried out in the gas phase by following the decomposition of toluene vapors in a recirculating batch reactor. The results are in agreement with the tests presented in this paper and will be discussed elsewhere in relation with a recent report [18].

4. Concluding remarks

Fair thickness uniformity was achieved along the reactor axis for three series of samples (Table 1). Thiele modulus, a convenient parameter to predict the quality of infiltration, decreases sharply when lowering the pressure from 20 to 1 Torr. Infiltration is more efficient by lowering the temperature at 300°C but the ensuing compact, big-sized grain morphology (Fig. 5a) is less favorable to photocatalytic activity (Fig. 6). At 400°C and 20 Torr, the growth mode is definitely columnar (Fig. 4). The resulting high porosity and specific surface area are suitable for photocatalytic properties. But these experimental conditions yield poor infiltration through the glass tissue. The photocatalytic activity was comparatively measured for the three series of samples by evaluating the initial decomposition rates of Orange G, normalized by the mass of the deposited

photocatalyst (Table 1). Sample 2 is the most active although the TiO_2 film exhibits a rather compact and unfavorable morphology. This can be explained by the most efficient infiltration (good uniformity and conformal coverage), which leads to a higher active surface area (greater number of catalytic sites). Sample 3 exhibits intermediate characteristics and, as a result, an intermediate photocatalytic activity is observed indicating that the infiltration efficiency is a major factor. Further works are in progress to optimize this CVI process for a one step production of supported photocatalysts.

Acknowledgements

Authors thank B.W. Sheldon (Brown University, Providence) and N. Reuge (LGC, Toulouse) for fruitful discussions on CVI technique, J. M. Herrmann, C. Guillard and E. Puzenat (IRCELYON, Lyon) for collaboration and discussions on gas phase photocatalysis, D. Truyen (CIRIMAT, Toulouse) for B.E. T measurements.

References

- [1] S.M. Gupte, J.A. Tsamopoulos, *J. Electrochem. Soc.* 136 (1989) 555.
- [2] N. Popovska, D.A. Streitwieser, C. Xu, H. Gerhard, *J. Eur. Ceram. Soc.* 25 (2005) 829.
- [3] G.L. Vignoles, F. Langlais, C. Descamps, A. Mouchon, H. Le Poche, N. Reuge, N. Bertrand, *Surf. Coat. Technol.* 188–189 (2004) 241.
- [4] H.C. King, M.C. Renier, K.E. Ellzey, W.J. Lackey, *Chem. Vap. Depos.* 9 (2003) 59.
- [5] H.C. Chang, T.F. Morse, B.W. Sheldon, *J. Am. Ceram. Soc.* 80 (1997) 1805.
- [6] J.M. Agullo, F. Maury, R. Morancho, *Thin Solid Films* 209 (1992) 52.
- [7] D. Robert, A. Piscopo, O. Heintz, J.V. Weber, *Catal. Today* 54 (1999) 291.
- [8] H. Okudera, Y. Yokogawa, *Thin Solid Films* 423 (2003) 119.
- [9] F.-D. Duminica, F. Maury, F. Senocq, *Surf. Coat. Technol.* 188/189 (2004) 255.
- [10] F.-D. Duminica, F. Maury, R. Hausbrand, *Surf. Coat. Technol.* (2007-this volume) <http://dx.doi.org/10.1016/j.surfcoat.2007.04.011>.
- [11] F.-D. Duminica, F. Maury, R. Hausbrand, *Surf. Coat. Technol.* <http://dx.doi.org/10.1016/j.surfcoat.2007.04.061>.
- [12] C. Sarantopoulos, F.D. Duminica, A.N. Gleizes, F. Maury, in: A. Devi, H. Parala, M.L. Hitchman, R.A. Fischer, M.D. Allendorf (Eds.), *Chem. Vap. Deposition XV, EUROCVI 15, Proc. volume PV 09, Electrochem. Soc., Pennington, NJ, 2005*, p. 252.
- [13] C.J. Taylor, D.C. Gilmer, D.G. Colombo, G.D. Wilk, S.A. Campbell, J. Roberts, W.L. Gladfelter, *J. Am. Chem. Soc.* 121 (1999) 5220.
- [14] K.L. Siefering, G.L. Griffin, *J. Electrochem. Soc.* 137 (1990) 814.
- [15] G.A. Battiston, R. Gerbasi, M. Porchia, L. Rizzo, *Chem. Vap. Depos.* 5 (1999) 73.
- [16] C. Sarantopoulos, A.N. Gleizes, F. Maury, E. Puzenat, C. Guillard, J.-M. Herrmann, *Chem. Vap. Deposition* (submitted for publication).
- [17] S.-C. Jung, B.-H. Kim, S.-J. Kim, N. Imaishi, Y.-I. Cho, *Chem. Vap. Depos.* 11 (2005) 137.
- [18] S.B. Kim, S.C. Hong, *Appl. Catal., B* 35 (2002) 305.